

Excellent microwave absorption property of the $\text{CoFe}_2\text{O}_4/\text{Y}_3\text{Fe}_5\text{O}_{12}$ ferrites based on graphene

Yaru Wang¹ · Yongping Pu¹ · Yu Shi¹ · Han Cui¹

Received: 30 March 2017 / Accepted: 9 May 2017 / Published online: 22 May 2017
© Springer Science+Business Media New York 2017

Abstract The graphene/ $\text{CoFe}_2\text{O}_4/\text{Y}_3\text{Fe}_5\text{O}_{12}$ nanocomposite were successfully synthesized by a deoxidation technique. The phase composition, morphology and electromagnetic properties of the composites were characterized by X-ray diffractometer, scanning electron microscope, X-ray photoelectron spectroscopy, Raman spectra, and vector network analyzer. The electromagnetic parameters of the graphene/ $\text{CoFe}_2\text{O}_4/\text{Y}_3\text{Fe}_5\text{O}_{12}$ nanocomposite were investigated in the 2–18 GHz range. The experimental results show that the graphene/ $\text{CoFe}_2\text{O}_4/\text{Y}_3\text{Fe}_5\text{O}_{12}$ nanocomposite exhibits evidently enhanced microwave absorbing performance in comparison with the $\text{CoFe}_2\text{O}_4/\text{Y}_3\text{Fe}_5\text{O}_{12}$ nanocomposite. An effective absorption band is obtained by graphene/ $\text{CoFe}_2\text{O}_4/\text{Y}_3\text{Fe}_5\text{O}_{12}$ nanocomposite at 14–16 GHz and the maximum reflection loss is -36.1 dB at 14.88 GHz.

1 Introduction

Microwave absorbing materials have attracted much attention due to their great potential in civilian application including protection people from electromagnetic radiation and their military purposes, such as radar invisible aircrafts, bombs and tanks [1–3]. Therefore, excellent microwave absorbing materials are required to be lightweight with strong absorption and broad absorption bandwidths. In recent years, conducting polymers, carbon nanotubes,

ferrites, etc. have been developed to attenuate electromagnetic wave [4–7].

Ferrites, as magnetic materials, have become a hot topic due to their low cost, environmental stability, high saturation magnetization and magnetic loss. The fundamental magnetic properties of $\text{Y}_3\text{Fe}_5\text{O}_{12}$ originates from the magnetic ions and their relationship to the surrounding oxygen ions. $\text{Y}_3\text{Fe}_5\text{O}_{12}$ has attracted much attention as memory materials and microwave device [8]. Simultaneously, the spinel ferrites CoFe_2O_4 have strong anisotropy, high saturation magnetization and moderate coercivity at room temperature [9]. However, ferrite absorbers have higher density and lower dielectric loss which restrain their wide applications as microwave absorbers. To overcome these shortcomings, dielectric loss fillers such as conduction polymers, graphene are always added into the system. Recently, graphene has grabbed considerable attention for microwave absorption due to the residual defects, the large aspect ratio, interfacial polarizations and high conductivity [10, 11].

In our work, the $\text{CoFe}_2\text{O}_4/\text{Y}_3\text{Fe}_5\text{O}_{12}$ nanocomposite powders were successfully synthesized by a sol–gel method, and then the $\text{CoFe}_2\text{O}_4/\text{Y}_3\text{Fe}_5\text{O}_{12}$ was deposited on the surface of graphene sheets. The samples can obtain good electrical conductivity and electromagnetic properties, achieving the optimized microwave absorption property.

2 Experimental procedure

2.1 Preparation of graphite oxide (GO)

GO was prepared by modified Hummers' method [12]. In a typical preparation, 2 g portion of natural flake graphite with 2 g of NaNO_3 , and 96 ml of concentrated H_2SO_4

✉ Yongping Pu
puyongping@sust.edu.com

¹ School of Materials Science & Engineering, Shaanxi University of Science and Technology, Xi'an 710021, China

were stirred together in an ice water bath, and then 12 g of KMnO_4 was slowly added to the above mixture for 1.5 h. After that, the solution was moved to a 35°C water bath and went on stirring for about 2 h to form a thick paste. 80 ml of distilled water was slowly added into the above paste and the resulting solution was stirred for 30 min while the temperature was raised to 90°C . Finally, 200 ml of water containing 10 ml of H_2O_2 was added for 10 min until the color of the solution turned from dark brown to yellow. The graphite oxide deposit was collected from the graphite oxide suspension by high-speed centrifugation, and repeatedly washed with distilled water until the pH value is 7 and then dried at 60°C .

2.2 Preparation of $0.7\text{CoFe}_2\text{O}_4/0.3\text{Y}_3\text{Fe}_5\text{O}_{12}$

$\text{CoFe}_2\text{O}_4/\text{Y}_3\text{Fe}_5\text{O}_{12}$ nanocomposite powder with a mass ratio of 3:7 was synthesized by a one-step sol–gel method. The aqueous solution was prepared by dissolving $\text{Y}(\text{NO}_3)_3 \cdot 6\text{H}_2\text{O}$, and $\text{Fe}(\text{NO}_3)_3 \cdot 9\text{H}_2\text{O}$, $\text{Co}(\text{NO}_3)_2 \cdot 6\text{H}_2\text{O}$, and $\text{C}_6\text{H}_8\text{O}_7 \cdot \text{H}_2\text{O}$ into distilled water and magnetically stirred at 80°C . Ammonia was added to the above solution to adjust the pH value to 7. After that the mixture solution was dried at 200°C for 2 h, the black floppy carbonaceous precursor powders were obtained. Finally, the precursor powders were calcined at 1100°C for 4 h to obtain the $0.7\text{CoFe}_2\text{O}_4/0.3\text{Y}_3\text{Fe}_5\text{O}_{12}$ nanocomposite powder.

2.3 Preparation of graphene/ $0.7\text{CoFe}_2\text{O}_4/0.3\text{Y}_3\text{Fe}_5\text{O}_{12}$

Graphene/ $0.7\text{CoFe}_2\text{O}_4/0.3\text{Y}_3\text{Fe}_5\text{O}_{12}$ nanocomposite powder was prepared with the mass ratio of GO and $0.7\text{CoFe}_2\text{O}_4/0.3\text{Y}_3\text{Fe}_5\text{O}_{12}$ is 1:5. In the first step, a certain amount of GO were dispersed in glycol by ultrasonication for 4 h. And then the $0.7\text{CoFe}_2\text{O}_4/0.3\text{Y}_3\text{Fe}_5\text{O}_{12}$ nanocomposite powder was added into the suspension. The suspension continued dispersing by ultrasonication for 1 h. After that, the mixture was reacted at 200°C for 24 h by a hydrothermal method. The resulted precipitate was filtrated, washed with distilled water and ethanol repeatedly and dried under vacuum at 50°C for about 24 h.

2.4 Characterization

The phase composition of the samples was detected by an X-ray diffractometer (XRD) with $\text{Cu K}\alpha$ radiation (Rigaku D/MAX-2400, Japan). The scanning electron microscope (SEM) (Hitachi S-4800, Japan) equipped with an energy dispersive X-ray spectroscopy (EDS). The chemical states were investigated by X-ray photoelectron spectroscopy (XPS, PHI 5300X). The Raman spectra of the nanocomposite samples were obtained using an inVia Laser-Raman spectrometer (Renishaw-inVia, England) with a 514 nm

radiation. The electromagnetic parameters were measured in a HP8753D vector network analyzer at frequency range of 2–18 GHz. The samples were pressed to be toroidal samples with the height about 3 mm according to the mass ratio 3:1 of paraffin and composite powders.

3 Results and discussion

The XRD patterns of the $\text{CoFe}_2\text{O}_4/\text{Y}_3\text{Fe}_5\text{O}_{12}$ nanocomposite and the graphene/ $\text{CoFe}_2\text{O}_4/\text{Y}_3\text{Fe}_5\text{O}_{12}$ nanocomposite are shown in Fig. 1. The results suggest that the characteristic peaks for the two phases of $\text{Y}_3\text{Fe}_5\text{O}_{12}$ and CoFe_2O_4 can be found in all samples and no any other phase can be detected. The XRD patterns are consistent with $\text{Y}_3\text{Fe}_5\text{O}_{12}$ phase (JCPDS 21-1450) and CoFe_2O_4 phase (JCPDS 22-1086). The diffraction peaks can be perfectly indexed to the cubic structure of $\text{Y}_3\text{Fe}_5\text{O}_{12}$ and the cubic spinel structure of CoFe_2O_4 . It shows that the introduction of graphene will not affect the crystalline structure during the reaction. Therefore, it can be concluded that the graphene/ $\text{CoFe}_2\text{O}_4/\text{Y}_3\text{Fe}_5\text{O}_{12}$ nanocomposite has been obtained during the reaction process, and the two phase of $\text{Y}_3\text{Fe}_5\text{O}_{12}$ and CoFe_2O_4 can be coexisted.

Raman spectroscopy is also one of the most sensitive and informative techniques to characterize disorder in sp^2 carbon materials. Figure 2 presents the Raman spectrum of graphite oxide and graphene/ $\text{CoFe}_2\text{O}_4/\text{Y}_3\text{Fe}_5\text{O}_{12}$ nanocomposite. The variation of the relative intensities of G (the E_{2g} mode of sp^2 carbon atoms) and D (the symmetry A_{1g} mode) bands in the Raman spectra of the graphene during the reduction usually reveals the change of the electronic conjugation state [13–16]. As depicted in the Fig. 2, the

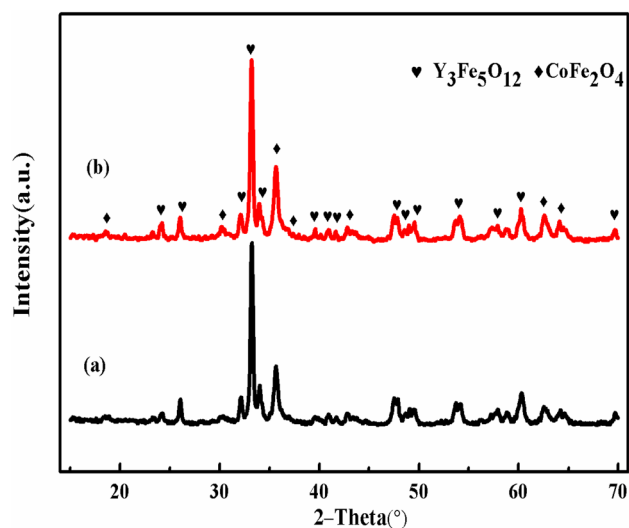


Fig. 1 XRD patterns of (a) $\text{CoFe}_2\text{O}_4/\text{Y}_3\text{Fe}_5\text{O}_{12}$ nanocomposite and (b) graphene/ $\text{CoFe}_2\text{O}_4/\text{Y}_3\text{Fe}_5\text{O}_{12}$ nanocomposite

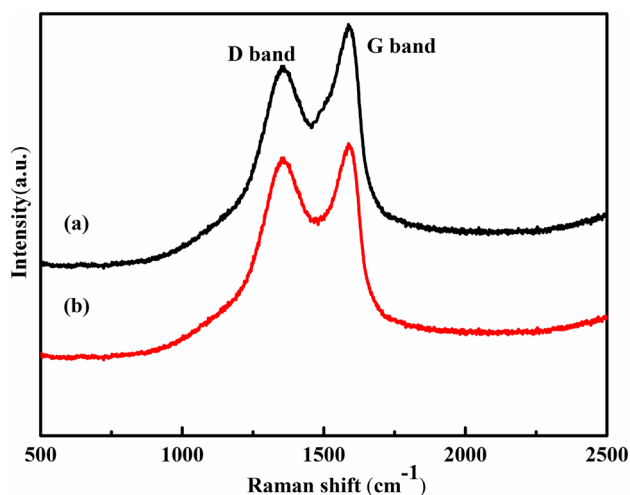


Fig. 2 Raman spectra of (a) graphite oxide and (b) graphene/ $\text{CoFe}_2\text{O}_4/\text{Y}_3\text{Fe}_5\text{O}_{12}$ nanocomposite

intensity ratio of D to G band (I_D/I_G) of graphene is 1.05 which is higher than of well-crystallized graphite oxide (0.93). This agrees well with the Raman spectrum of the graphene reduces by hydrazine that is reported by Stankovich et al. [13], indicating the reduction do take place.

Figure 3 show the SEM micrograph of the $\text{CoFe}_2\text{O}_4/\text{Y}_3\text{Fe}_5\text{O}_{12}$ nanocomposite and graphene/ $\text{CoFe}_2\text{O}_4/\text{Y}_3\text{Fe}_5\text{O}_{12}$ nanocomposite. Figure 3a shows the $\text{Y}_3\text{Fe}_5\text{O}_{12}$ and CoFe_2O_4 phases are well distributed. For graphene/ $\text{CoFe}_2\text{O}_4/\text{Y}_3\text{Fe}_5\text{O}_{12}$ in Fig. 3b, it can be observed that a continuous overlayer of conducting graphene can be formed on the ferrite particle surface. Figure 4 shows the EDS spectrum and the corresponding mapping result of the representative graphene/ $\text{CoFe}_2\text{O}_4/\text{Y}_3\text{Fe}_5\text{O}_{12}$ nanocomposite. It can be found that the whole area of the SEM picture

(Fig. 4 b) contains O, Fe, Y, Co and C five elements. The atomic ratio of Co to Y is 0.77, which is approximately equal to the nominal value of 0.78. The mass fraction of Y and Fe in the sample reaches 11.6 and 37.4%, respectively, while it is 7% for the element C. As shown in Fig. 4c, the O, Fe, Y, Co elements are well distributed in the picture, but the C element is distributed in the local area. In this area, the powder is surrounded by the graphene, so the C element is more concentrated than other area.

The overall XPS spectra of graphene/ $\text{CoFe}_2\text{O}_4/\text{Y}_3\text{Fe}_5\text{O}_{12}$ nanocomposite is shown in Fig. 5a. It can be clearly observed that five peaks corresponding to Y 3d, O 1s, Co 2p, Fe 2p, and C 1s appear in the sample. The reduction of graphene oxide is also characterized using XPS spectra and Raman spectra. Figure 5b shows the C 1s XPS spectra of graphene/ $\text{CoFe}_2\text{O}_4/\text{Y}_3\text{Fe}_5\text{O}_{12}$ nanocomposite. The peaks 1, 2, and 3 correspond to C=C/C–C in aromatic rings, C–O (epoxy and alkoxy), and C=O, groups, respectively [15]. After the reduction of graphene, the intensities of all C 1s peaks of the carbons binding to oxygen, especially the peak of C–O (epoxy and alkoxy), decreases dramatically, revealing that most oxygen containing functional groups are removed after reduction.

Figure 6 shows frequency dependence of the complex permittivity, complex permeability and loss tangent of dielectric/magnetic of the samples between 2 and 18 GHz. As we all known, the ϵ' and μ' values stand for storage ability of electromagnetic energy while the ϵ'' and μ'' values stand for the dissipation of energy. It can be observed from Fig. 6a, b that ϵ' and ϵ'' values of graphene/ $\text{CoFe}_2\text{O}_4/\text{Y}_3\text{Fe}_5\text{O}_{12}$ nanocomposite increase while the μ' and μ'' values decrease after the introduction of graphene, which is due to the fact that the addition of graphene enlarges the interface of graphene/ $\text{CoFe}_2\text{O}_4/\text{Y}_3\text{Fe}_5\text{O}_{12}$ nanocomposite and makes the dipole and interfacial polarizability of

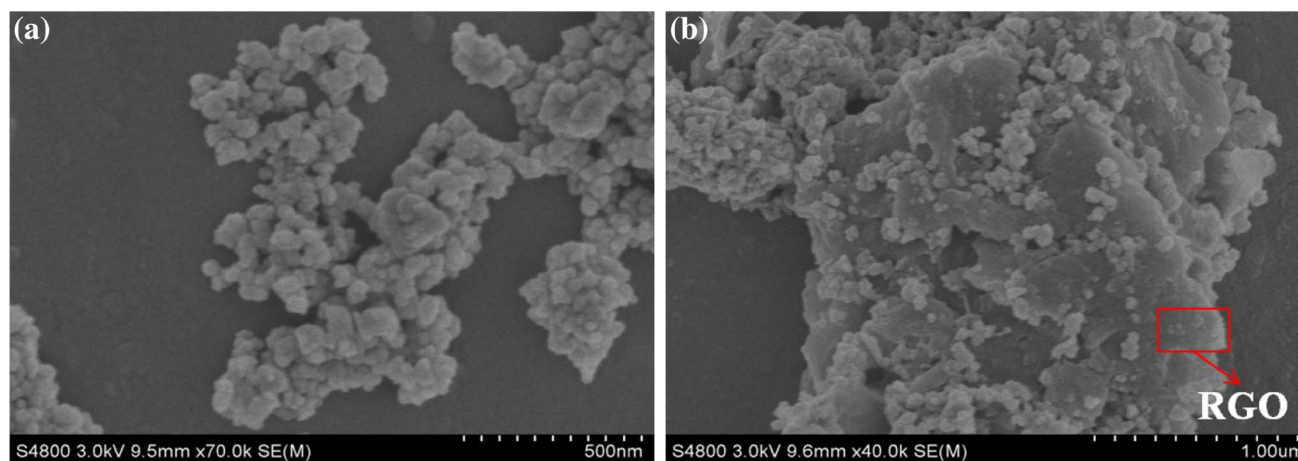


Fig. 3 SEM micrographs of a $\text{CoFe}_2\text{O}_4/\text{Y}_3\text{Fe}_5\text{O}_{12}$ nanocomposite and b graphene/ $\text{CoFe}_2\text{O}_4/\text{Y}_3\text{Fe}_5\text{O}_{12}$ nanocomposite

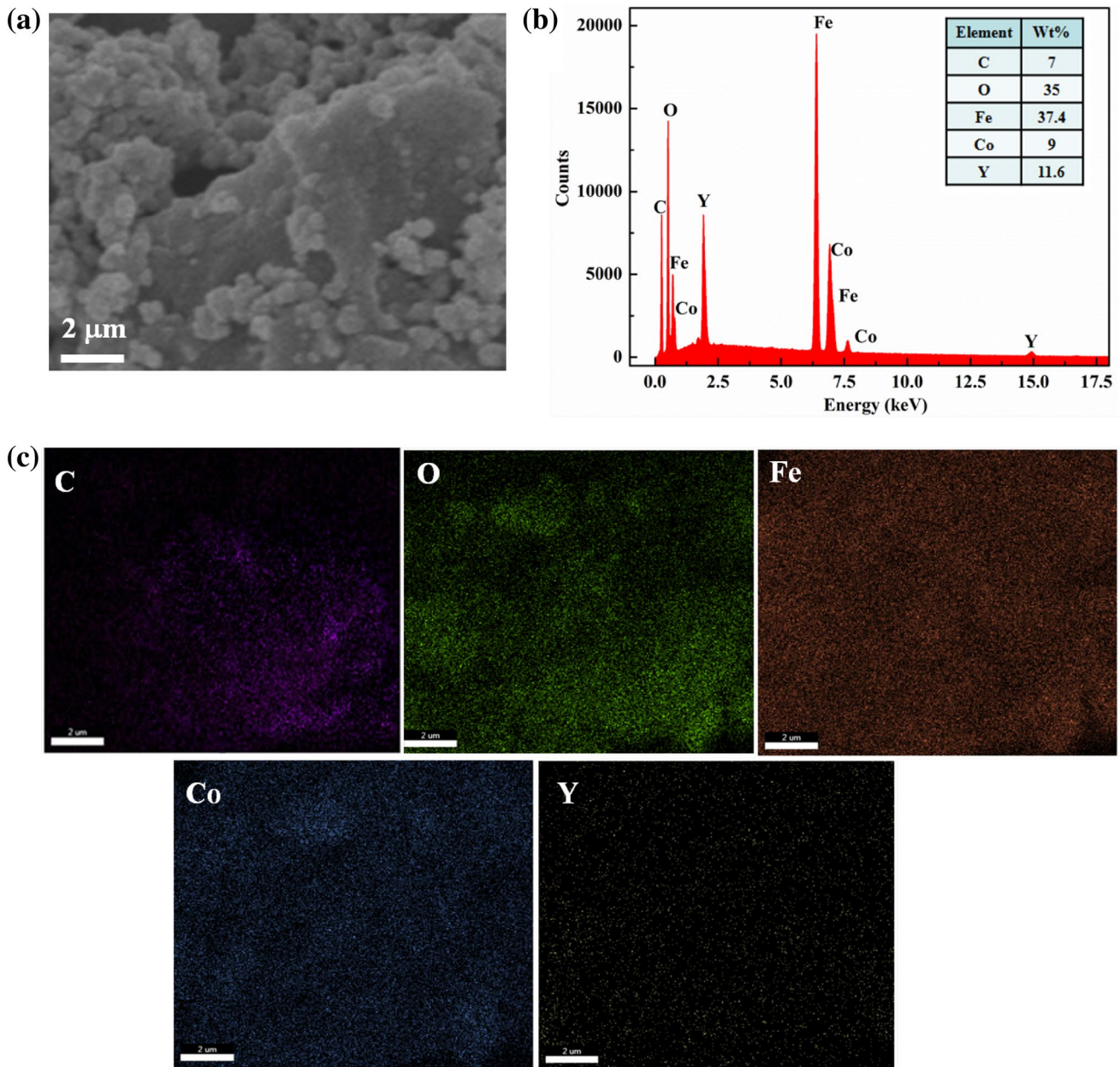


Fig. 4 SEM micrograph and EDS mapping analysis result of the representative graphene/CoFe₂O₄/Y₃Fe₅O₁₂ nanocomposite: **a** the SEM of graphene/CoFe₂O₄/Y₃Fe₅O₁₂ nanocomposite; **b** the data of gra-

phene/CoFe₂O₄/Y₃Fe₅O₁₂ nanocomposite EDS mapping analysis; **c** the mapping analysis of five elements distribution pictures

the nanocomposite enhanced in the electromagnetic field, which results in the larger dielectric loss and smaller magnetic loss [17].

In order to investigate microwave absorption properties, the reflection loss (RL) of CoFe₂O₄/Y₃Fe₅O₁₂ and graphene/CoFe₂O₄/Y₃Fe₅O₁₂ nanocomposite are calculated by the following equations:

$$RL(dB) = 20 \lg \left| \frac{Z_{in} - 1}{Z_{in} + 1} \right| \tag{1}$$

$$Z_{in} = \sqrt{\frac{\mu_r}{\epsilon_r}} \tanh \left(j \frac{2\pi f d}{c} \sqrt{\mu_r \epsilon_r} \right) \tag{2}$$

where Z_{in} is the input impedance of the absorber, c is the velocity of electromagnetic wave in vacuum, f is the frequency and d is the layer thickness, ϵ_r and μ_r are the complex relative permittivity and permeability, respectively.

The calculated reflection loss curves of the samples are shown in Fig. 7. It is clearly seen that there is nearly

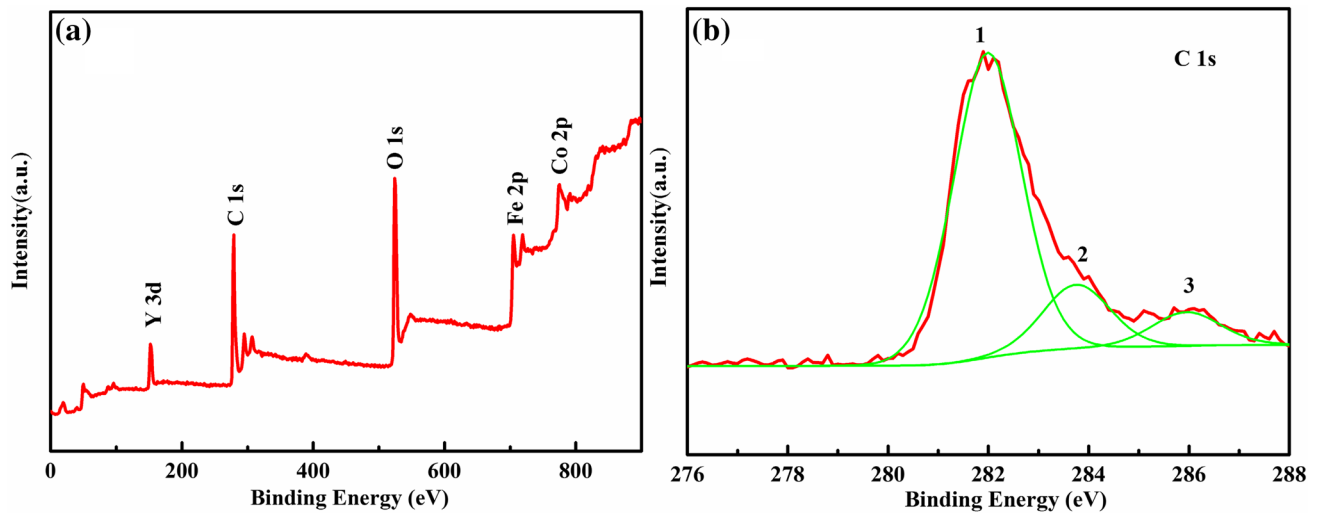


Fig. 5 a Overall XPS spectra of graphene/CoFe₂O₄/Y₃Fe₅O₁₂ nanocomposite; b C 1s XPS graphene/CoFe₂O₄/Y₃Fe₅O₁₂ nanocomposite

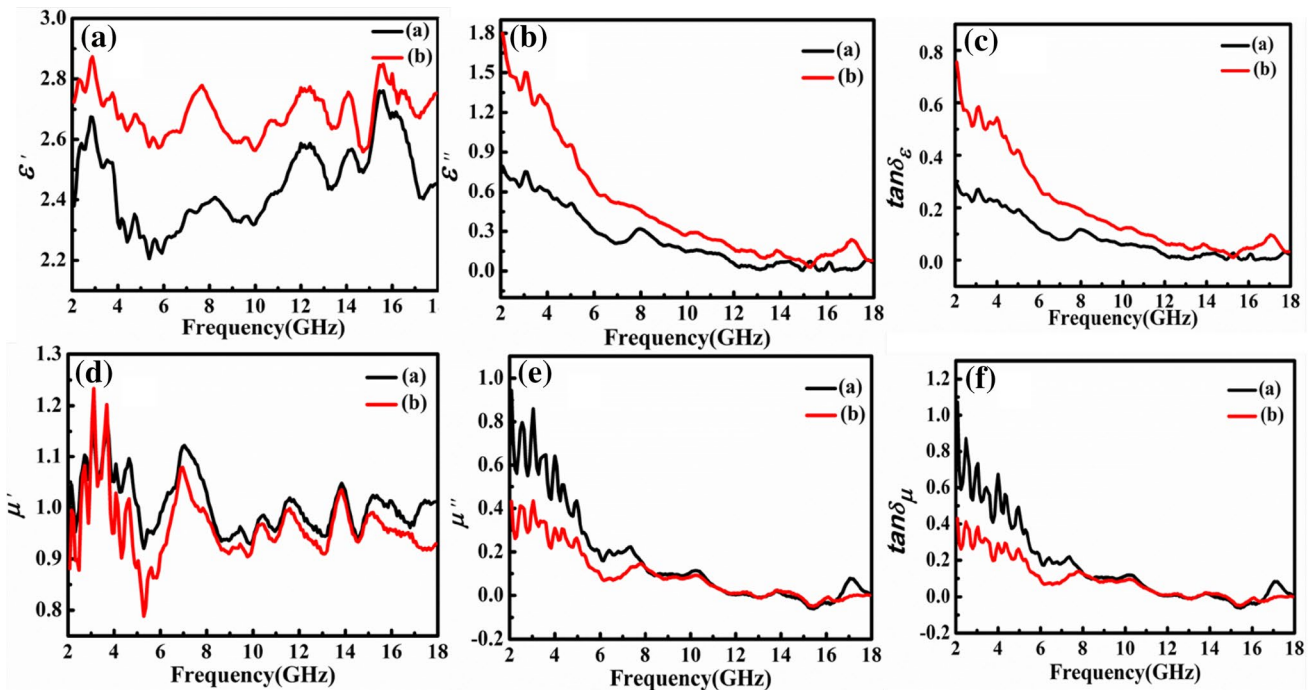


Fig. 6 a–f Frequency dependence of real and imaginary parts of the complex permittivity and the complex permeability of (a) CoFe₂O₄/Y₃Fe₅O₁₂ nanocomposite and (b) graphene/CoFe₂O₄/Y₃Fe₅O₁₂ nanocomposite

no broad peak with a bandwidth lower than -15 dB for CoFe₂O₄/Y₃Fe₅O₁₂ nanocomposite. However, the introduction of graphene can significantly enhance the microwave absorbing abilities. An effective absorption band is obtained at 14–16 GHz and the maximum reflection loss is -36.1 dB at 14.88 GHz. The strong attenuation characteristics of microwave absorbing materials must satisfy a proper matching of the magnetic loss and dielectric loss [18]. CoFe₂O₄/Y₃Fe₅O₁₂ nanocomposite can not achieve

the matching of the magnetic loss and dielectric loss. Compared with this, the graphene/CoFe₂O₄/Y₃Fe₅O₁₂ nanocomposite possess more proper matching of the magnetic loss and dielectric loss and larger microwave absorbing ability is obtained consequently. The addition of graphene can well balance the magnetic loss and the dielectric loss, and reduces the magnetic-coupling effect between grains, while increase the effective surface anisotropy of the grains [19]. Above these reasons make

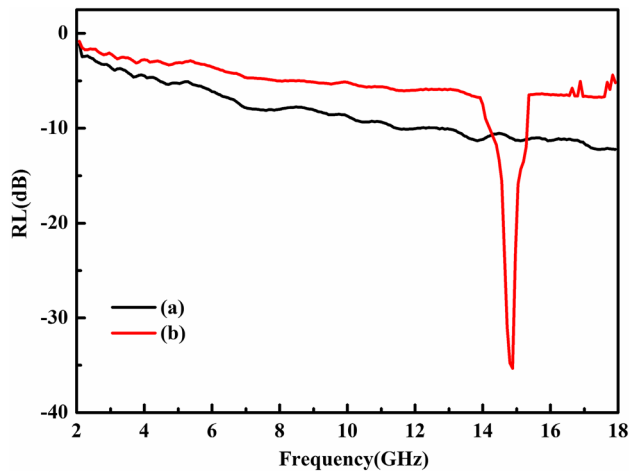


Fig. 7 Reflection loss curves of the samples: (a) $\text{CoFe}_2\text{O}_4/\text{Y}_3\text{Fe}_5\text{O}_{12}$ nanocomposite and (b) graphene/ $\text{CoFe}_2\text{O}_4/\text{Y}_3\text{Fe}_5\text{O}_{12}$ nanocomposite

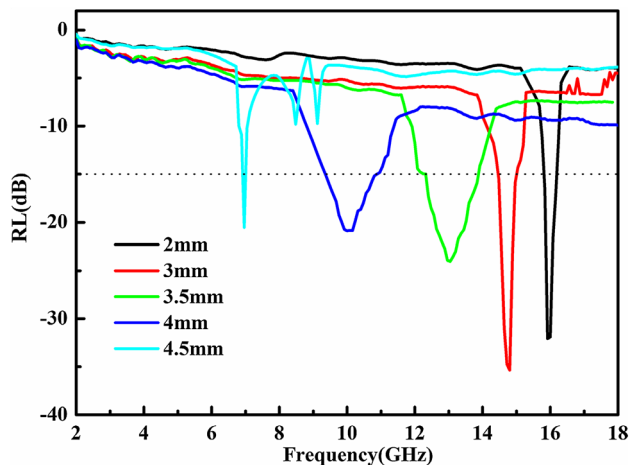


Fig. 8 Reflection loss curves in 2–18 GHz for graphene/ $\text{CoFe}_2\text{O}_4/\text{Y}_3\text{Fe}_5\text{O}_{12}$ nanocomposite with different specimen thicknesses

the graphene/ $\text{CoFe}_2\text{O}_4/\text{Y}_3\text{Fe}_5\text{O}_{12}$ nanocomposite have enhanced microwave absorption properties, becoming the candidate for the good microwave absorbing materials.

The microwave absorption performance can be mainly related to the specimen thickness effect [20]. The calculated microwave reflection loss in 2–18 GHz for graphene/ $\text{CoFe}_2\text{O}_4/\text{Y}_3\text{Fe}_5\text{O}_{12}$ nanocomposite with different specimen thicknesses is shown in Fig. 8. It is found that the peak values shifts to a lower frequency with specimen thickness increase. The reflection loss values exceeding -30 dB can be obtained by tuning the specimen thickness between 3 and 2 mm. This affirms that the thickness of the sample also plays a major role in the microwave absorption performance of the sample.

4 Conclusions

The graphene/ $\text{CoFe}_2\text{O}_4/\text{Y}_3\text{Fe}_5\text{O}_{12}$ nanocomposite were successfully synthesized by a deoxidation technique. XRD and SEM studies have established formation of the graphene/ $\text{CoFe}_2\text{O}_4/\text{Y}_3\text{Fe}_5\text{O}_{12}$ nanocomposite. The Raman and XPS measurements shows the reduction of the graphene, which has good electrical conductivity properties. Our results indicate that the graphene/ $\text{CoFe}_2\text{O}_4/\text{Y}_3\text{Fe}_5\text{O}_{12}$ nanocomposite exhibits good absorption performances and the maximum reflection loss of the nanocomposite can reach to -36.1 dB. Therefore, the prepared graphene/ $\text{CoFe}_2\text{O}_4/\text{Y}_3\text{Fe}_5\text{O}_{12}$ nanocomposite becomes potential candidate in microwave absorbing field.

Acknowledgements This research was supported by the National Natural Science Foundation of China (51372144) and the Key Program of Innovative Research Team of Shaanxi Province (2014KCT-06).

References

1. R. Qiang, Y.C. Du, Y. Wang, N. Wang, C.H. Tian, J. Ma, P. Xu, X.J. Han, Rational design of yolk-shell C@C microspheres for the effective enhancement in microwave absorption. *Carbon* **98**, 599–606 (2016)
2. J.W. Liu, R.C. Che, H.J. Chen, F. Zhang, F. Xia, Q.S. Wu, M. Wang, Microwave absorption enhancement of multifunctional composite microspheres with spinel Fe_3O_4 cores and anatase TiO_2 shell. *Small* **8**, 1214–1221 (2012)
3. J.T. Feng, Y.C. Wang, Y.H. Hou, J.B. Li, L.C. Li, Synthesis and microwave absorption properties of coiled carbon nanotubes/ CoFe_2O_4 composites. *Ceram. Int.* **42**, 17814–17821 (2016)
4. Y. Zhao, H. Fan, K. Fu, L. Ma et al., Intrinsic electric field assisted polymeric graphitic carbon nitride coupled with $\text{Bi}_4\text{Ti}_3\text{O}_{12}/\text{Bi}_2\text{Ti}_2\text{O}_7$ heterostructure nanofibers toward enhanced photocatalytic hydrogen evolution. *Int. J. Hydrog. Energy* **41**, 16913–16926 (2016)
5. X. Ren, H. Fan, Y. Zhao, Z. Liu, Flexible Lead-Free $\text{BiFeO}_3/\text{PDMS}$ -Based Nanogenerator as Piezoelectric Energy Harvester. *ACS. Appl. Mater. Interfaces* **8**, 26190–26197 (2016)
6. L. Ma, H. Fan, H. Tian, J. Fang, X. Qian, The $n\text{-ZnO}/n\text{-In}_2\text{O}_3$ heterojunction formed by a surface-modification and their potential barrier-control in methanal gas sensing. *Sens. Actuators B-Chem.* **222**, 508–516 (2016)
7. N. Song, H. Fan, H. Tian, Reduced graphene oxide/ ZnO nanohybrids: metallic Zn powder induced one-step synthesis for enhanced photocurrent and photocatalytic response. *Appl. Surf. Sci.* **353**, 580–587 (2015)
8. H.B. Yang, T. Ye, Y. Lin, et al, Exchange coupling behavior and microwave absorbing property of the hard/soft ($\text{BaFe}_{12}\text{O}_{19}/\text{Y}_3\text{Fe}_5\text{O}_{12}$) ferrites based on polyaniline. *Synth. Met.* **210**, 245–250 (2015)
9. Y. Lin, P. Kang, H.B. Yang, M. Liu, Enhanced magnetoelectric properties of the laminated $\text{BaTiO}_3/\text{CoFe}_2\text{O}_4$. *J. Alloys. Compd.* **644**, 390–397 (2015)
10. J.J. Liang, Y. Wang, Y. Huang, Y.F. Ma, Z.F. Liu, J.M. Cai et al., Electromagnetic interference shielding of graphene/epoxy composites. *Carbon* **47**, 922–925 (2009)

11. M.S. Cao, X.X. Wang, W.Q. Cao, J. Yuan, Ultrathin graphene: electrical properties and highly efficient electromagnetic interference shielding. *J. Mater. Chem. C*, **3**, 6589–6599 (2015)
12. W.S. Hummers, R.E. Offeman, Preparation of graphitic oxide. *J. Am. Chem. Soc.* **80**, 1339–1339 (1958)
13. S. Stankovich, D.A. Dikin, R.D. Piner, K.A. Kohlhaas, A. Kleinhammes et al., Synthesis of graphene-based nanosheets via chemical reduction of exfoliated graphite oxide. *Carbon* **45**, 1558–1565 (2007)
14. F. Tuinstra, J.L. Koenig, Raman spectrum of graphite. *J. Chem. Phys.* **53**, 1126–1130 (1970)
15. J.L. Zhang, H.J. Yang, G.X. Shen, P. Cheng, J.Y. Zhang, S.W. Guo, Reduction of graphene oxide via L-ascorbic acid. *Chem. Comm.* **46**, 1112–1114 (2010)
16. Y.X. Ma, Y.F. Li, G.H. Zhao, L.Q. Yang, J.Z. Wang, X. Shan, X. Yan, Preparation and characterization of graphite nanosheets decorated with Fe₃O₄ nanoparticles used in the immobilization of glucoamylase. *Carbon* **50**, 2976–2986 (2012)
17. Y. Wang, Y. Huang, Q.F. Wang, M. Zong, Preparation and electromagnetic properties of graphene-supported Ni_{0.8}Zn_{0.2}Ce_{0.06}Fe_{1.94}O₄ nanocomposite. *Powder Technol.* **249** (2013) 304–308.
18. P. Xu, X.J. Han, C. Wang, D.H. Zhou, Z.S. Lv, A.H. Wen, X.H. Wang, B. Zhang, Synthesis of electromagnetic functionalized nickel/polypyrrole core/shell composites. *J. Phys. Chem. B*, **112**, 10443–10448 (2008)
19. Y.B. Li, G. Chen, Q.H. Li, G.Z. Qiu, X.H. Liu, Facile synthesis, magnetic and microwave absorption properties of Fe₃O₄/polypyrrole core/shell nanocomposite. *J. Alloys. Compd.* **509**, 4104–4107 (2011)
20. X.Q. Shen, F.Z. Song, J. Xiang, M.Q. Liu, Y.W. Zhu, Y.D. Wang, Shape anisotropy, exchange-coupling interaction and microwave absorption of hard/soft nanocomposite ferrite microfibers. *J. Am. Ceram. Soc.* **95**, 3863–3870 (2012)